European Polymer Journal 47 (2011) 88–97

Contents lists available at ScienceDirect

European Polymer Journal

journal homepage: www.elsevier.com/locate/europolj

On the deformation induced order–disorder transitions in the crystalline phase of polyamide 6

V. Miri *, O. Persyn, R. Seguela, J.M. Lefebvre

Unité Matériaux Et Transformations, UMR CNRS 8207, Université des Sciences et Technologies de Lille, Bât. C6, 59 655 Villeneuve d'Ascq, France

ARTICLE INFO

Article history:
Received 12 May 2010
Accepted 20 September 2010
Available online 8 October 2010

Keywords:
Nylon 6
Crystalline phase transitions
X-ray diffraction
FTIR spectroscopy

ABSTRACT

The present paper deals with the mechanically induced structural changes in polyamide 6 with initial α or γ crystal phases. By combining Wide Angle X-ray Scattering with FTIR spectroscopy measurements, order–disorder transitions have been clearly evidenced at 70 °C in both cases. The origin of this phenomenon is ascribed to structural defects involved in plastic deformation. By contrast, at 150 °C, no major transformation is revealed in α phase, whereas when starting from γ crystals, a γ–α transition is clearly evidenced. The central role of intracrystalline molecular mobilities is pointed out to account for the observed behaviours as a function of temperature.

1. Introduction

Strain-induced crystal phase transitions in semi-crystalline polymers have been the subject of numerous papers in the past years (see e.g. [1–3] and references therein). Such phenomena have been recognized to strongly influence the overall drawing behaviour, either by promoting ductility or on the contrary in some instances, by inducing premature embrittlement. Strain-induced phase transitions may be classified in different ways. From a conformational point of view, different situations may be encountered. In the case of martensitic phase transformations, deformation is accommodated by crystallographic cell change without modification of the chain conformation. A typical example is the case of polyethylene with the occurrence of an orthorhombic to monoclinic phase transition under uniaxial compression [4]. By contrast, some crystalline transformations involve conformational changes, as reported for polyvinylidene fluoride where the α to β phase transition under tension is related to a change from trans-gauche to all trans conformation [5]. Such a situation is also encountered in the case of syndiotactic PP (sPP) which displays a transition from a helical form into a trans-planar phase [6]. From a crystallographic point of view, the material can experience a disorder–order transition under stretching: phase transformation may imply reordering of a metastable (eventually mesomorphous) phase into a more stable crystalline organization as it is the case for the smectic form of isotactic polypropylene (iPP) which turns into the stable monoclinic α phase upon drawing [3]. The reverse situation is also encountered in which plastic deformation involve partial transformation of the stable crystal form into a less ordered and less stable structure. In iPP deformed by uniaxial compression, a α crystal-smectic phase transition has been also evidenced at temperature well above the stability limit of the disordered phase [7]. Globally, these solid-state processes depend on the thermo-mechanical processing history, molecular mobility in crystalline phase, crystal defects and stability. De Rosa et al. have studied the polymorphic transformations of iPP and sPP under tensile deformation as the function of chain microstructure [8,9]. They reported phase diagrams of both polymers where the stability domains of the different polymorphic forms are defined as a function of the degree of stereoregularity and deformation. Moreover, these authors conclude that the phase transitions are probably strain controlled rather than stress controlled and the value of the critical strain

* Corresponding author. Tel.: +33 (0) 3 20 33 64 16; fax: +33 (0) 3 20 43 65 91.
E-mail address: valerie.miri@univ-lille1.fr (V. Miri).

0014-3057/$ - see front matter © 2010 Elsevier Ltd. All rights reserved.
doi:10.1016/j.eurpolymj.2010.09.006

corresponding to the structural transitions depends on stereoregularity.

In the specific case of hydrogen-bonded polymers such as ethylene–vinyl alcohol copolymers (EVOH) or polyamide 6 (PA6), the monoclinic stable crystal phases display sheet-like structures incorporating the H bonds, while inter sheet interactions are of the van der Waals type. This crystalline organization is rather prejudicial to drawability, especially in the case of biaxial drawing processes which are widely developed (used) for film packaging applications. Therefore, a crucial issue is to understand the respective roles of initial crystal structure, molecular mobility and experimental conditions on the solid-state drawability of such polymers.

The case of PA6 is rather complex due to polymorphism. Depending on the melt processing conditions, the presence and nature of nucleating agents, several crystalline phases may coexist in the polymer film prior to be submitted to solid-state drawing processes. This situation is well documented [10–17]: two monoclinic phases with sheet-like structure are identified, namely the α and γ forms, together with a metastable β phase mostly described with a random distribution of H bonds and pseudo-hexagonal symmetry. According to [10–11], the chains are in an all-trans-planar conformation in the α phase, whereas the amide groups are twisted with respect to the methylene sequence in trans conformation in the γ phase. In the β phase, the situation is more ambiguous. From X-ray study, it seems however, that chain conformation looks like in the γ phase with amide group not coplanar to the methylene segments [13–16]. The α and γ forms are roughly thermally stable in contrast to the β phase that transforms into the α phase upon annealing and/or drawing [17–21]. Using a combination of X-ray diffraction and FTIR spectroscopy, a quantification of the mechanically induced β–α transition as a function of draw temperature and strain has been reported in pure PA6, as well as in miscible blends of PA6 with a semi-aromatic amorphous copolyamide [22]. As a general trend, it was shown that the constrained amorphous phase located at the crystal surface plays a major role on the reorganization capability of the crystalline phase towards its stable form. The disorder–order phase transition is only observed if the draw temperature is higher than the upper temperature limit of the viscoelastic relaxation peak associated with the activation of chain mobility in the constrained amorphous phase.

Owing to the polymorphism mentioned above, the case of PA6 is reconsidered in the present paper in a simplified manner with the aim to check the mechanical stability of the "pure" α or γ crystalline forms obtained by appropriate pretreatments of PA6 films. Phase change quantification is performed as a function of strain at various temperatures using X-ray diffraction, FTIR spectroscopy and thermal analysis.

2. Experimental

2.1. Preparation of samples

The polyamide-6 supplied by DSM (Akulon F136) has a weight-average molecular weight M_w = 50,000 g/mol. Microtalc is present as nucleant. PA6 was extruded at 275 °C into cast films about 80 μm thick on a chill roll at 22 °C. This processing resulted in predominant mesomorphous β phase. The so-called pure α phase samples were prepared by immersing films in superheated water at 150 °C in an autoclave for 40 min [17]. Pure γ phase samples were obtained through a reversible iodine treatment as described in literature [11]. The initial crystallinity of αPA6 and γPA6 has been estimated to 30 ± 2% by DSC experiments, using the melting enthalpy $\Delta H_f^0 = 230$ J/g whatever the crystalline form [23].

All samples were drawn in the dry state. Tensile specimens with 25 mm gauge length and 5 mm width have been stretched at a constant crosshead speed of 50 mm/min in the temperature range $70 < T < 150$ °C, up to nominal strains of about 3.5 at the maximum draw temperature. All structural characterizations refer to the local strain, ε, determined *a posteriori* from the spacing of ink marks printed 1.5 mm apart on the samples prior to deformation.

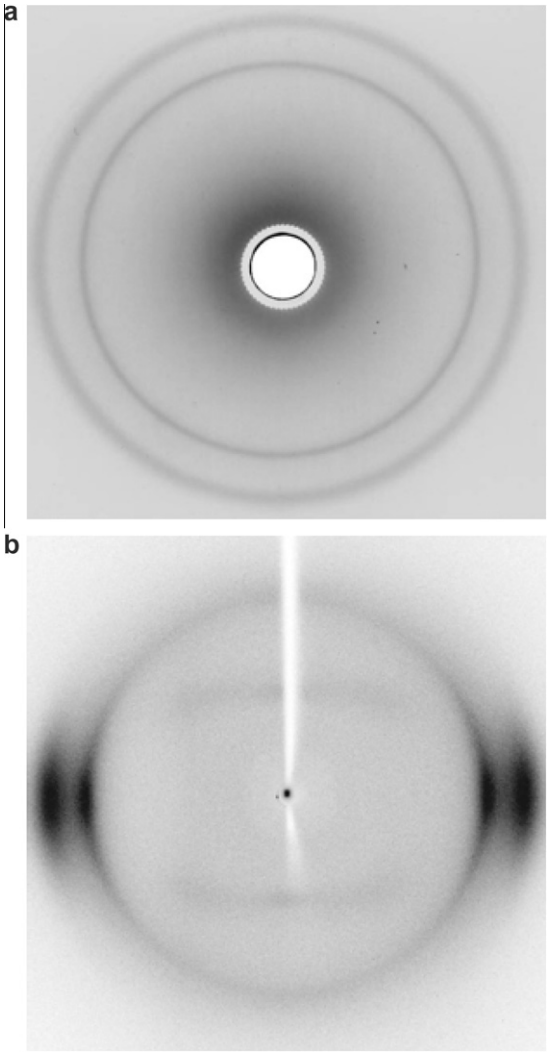

Fig. 1. Xray patterns of αPA6 (a) isotropic and (b) stretched at 70 °C ε = 2.1. (Vertical draw direction).

2.2. Structural characterizations

The drawn samples were analyzed unloaded at room temperature. 2D Wide Angle X-ray Scattering (WAXS) patterns were collected on a MAR345 Image plate detector, with CuK_α radiation ($\lambda = 1.54$ Å) produced by a Bruker-Nonius FR591 rotating-anode generator equipped with an Osmic's confocal Max-flux optical system and running at 100 mA and 50 kV. X-ray diffraction profiles were also recorded on a diffractometer equipped with a curved position-sensitive X-ray multidetector INEL CPS120. Uniaxially stretched films were fixed on the goniometer. The

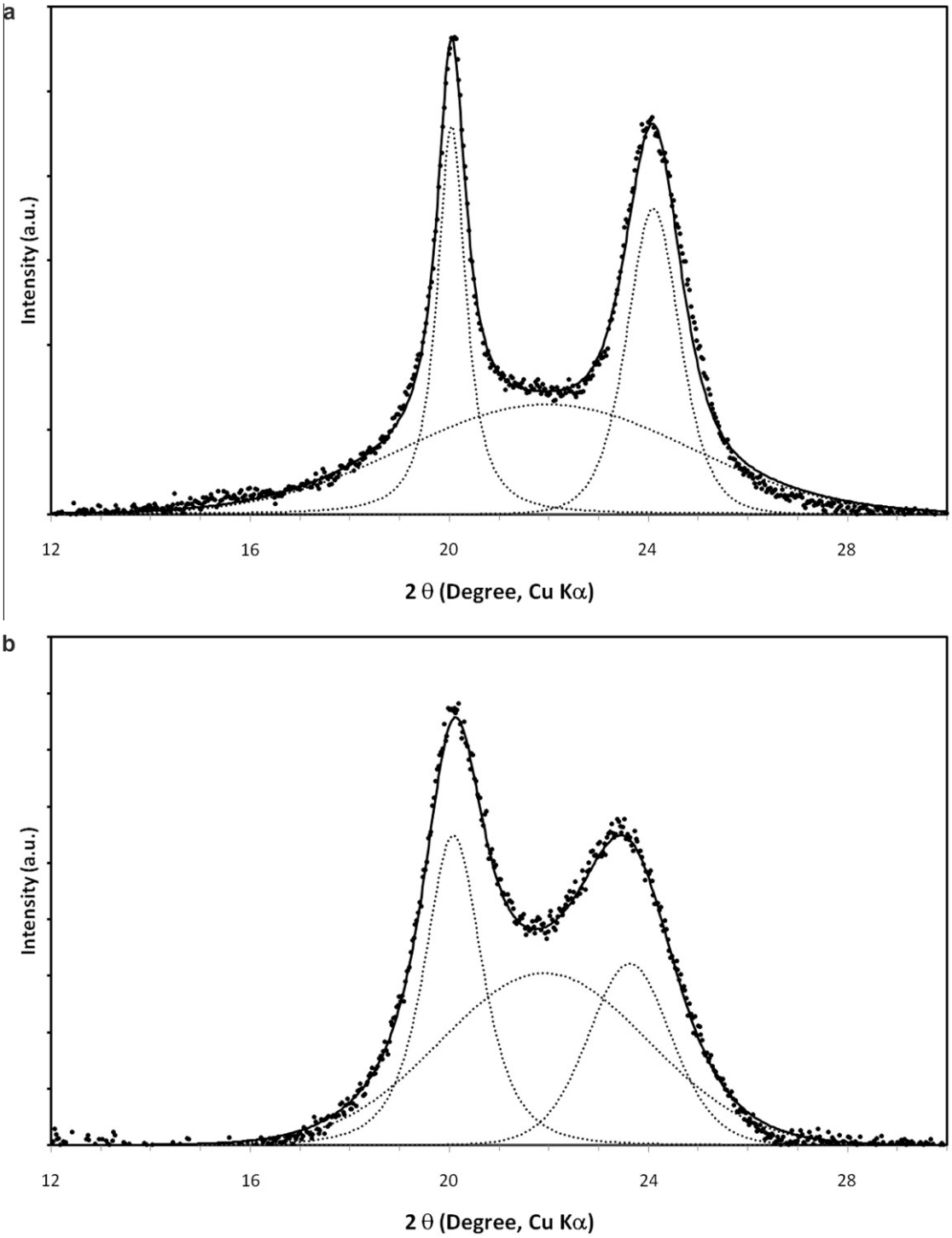

Fig. 2. Equatorial X-ray intensity profile of αPA6: (a): isotropic; (b): stretched at 70 °C, $\varepsilon = 2.1$.

Table 1
X-ray scattering parameters for αPA6.

			α	
		Amorphous	(2 0 0)	(0 0 2) + (2 0 2)
Isotropic	2θ	21.97	20.04	24.10
	FWHM	6.77	0.68	1.25
Stretched (70 °C; ε = 2.1)	2θ	21.91	20.08	23.62
	FWHM	4.91	1.35	1.96

diffraction data were collected in the equatorial plane in the range $12° < 2\theta < 30°$ with a step interval of about 0.03°. To elucidate the structural evolution, a deconvolution of the $I(2\theta)$ intensity profiles was performed using Peakfit software. Contributions of the amorphous and crystalline phases were approximated by Pearson VII functions. The apparent crystallite size (ACS) was estimated using the Scherrer equation:

$$ACS = \frac{0.9\lambda}{(\Delta 2\theta)\cos\theta} \quad (1)$$

where λ is the X-ray wavelength, $(\Delta 2\theta)$ is the full-width at half-maximum (FWHM) of the crystalline peak, and 2θ is the peak position [24]. In the case of α crystals, the (2 0 0) and (0 0 2) reflections were used to calculate the crystallite size along the hydrogen-bonded direction *a*, and along the *c* axis, respectively.

FTIR experiments were carried out to quantify crystal phase evolution as a function of thermomechanical history, following the procedure already detailed elsewhere [25]. Unpolarized FTIR spectra have been determined in order to overcome orientation effects for quantitative assessment of crystal content. Spectra were recorded over the wave number range 850–1150 cm^{-1} with a resolution of 2 cm^{-1}. The spectrum intensity was normalized with respect to film thickness.

Table 2
Crystallite dimensions along a and c axes for isotropic and stretched αPA6.

	Crystallite size (Å)	
	a direction	*c* direction
Isotropic	119	65
Stretched (70 °C; ε = 2.1)	60	41

DSC experiments have been carried out on a Perkin–Elmer DSC-7 apparatus on carefully dried samples. Temperature was calibrated using high purity indium and zinc samples. The heating rate was 10 °C/min and the sample weight was about 10 mg.

3. Results

3.1. The case of "pure" α PA6

Fig. 1 compares the 2D WAXS patterns of αPA6 samples prior and after stretching at 70 °C. The isotropic sample is

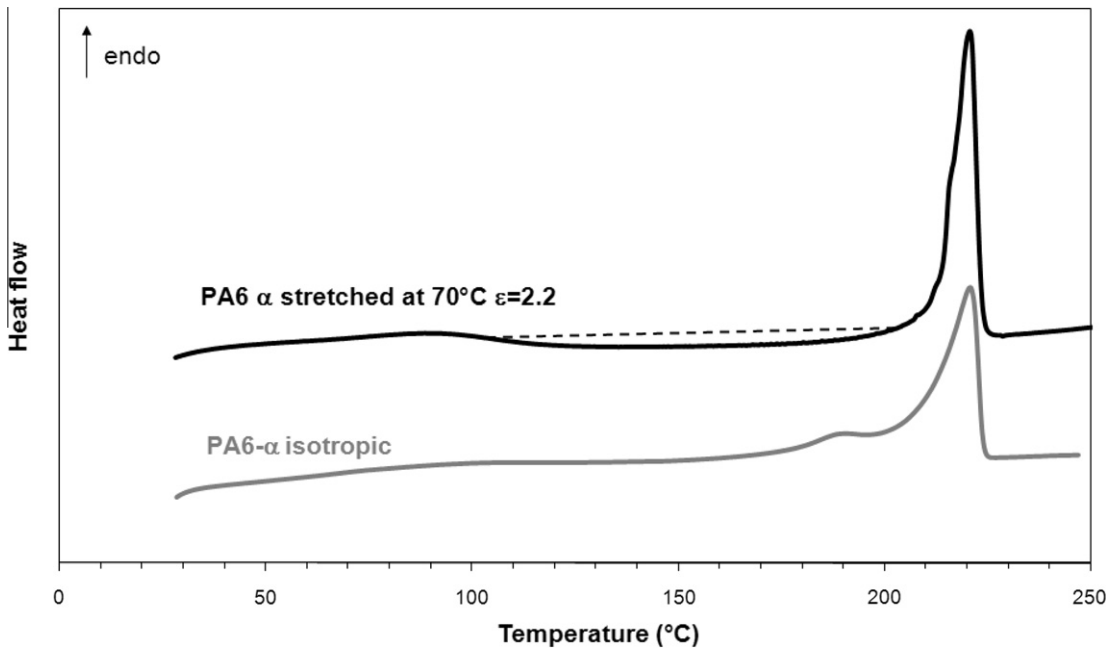

Fig. 3. DSC thermograms for αPA6, isotropic and stretched up to ε = 2.2 at 70 °C.

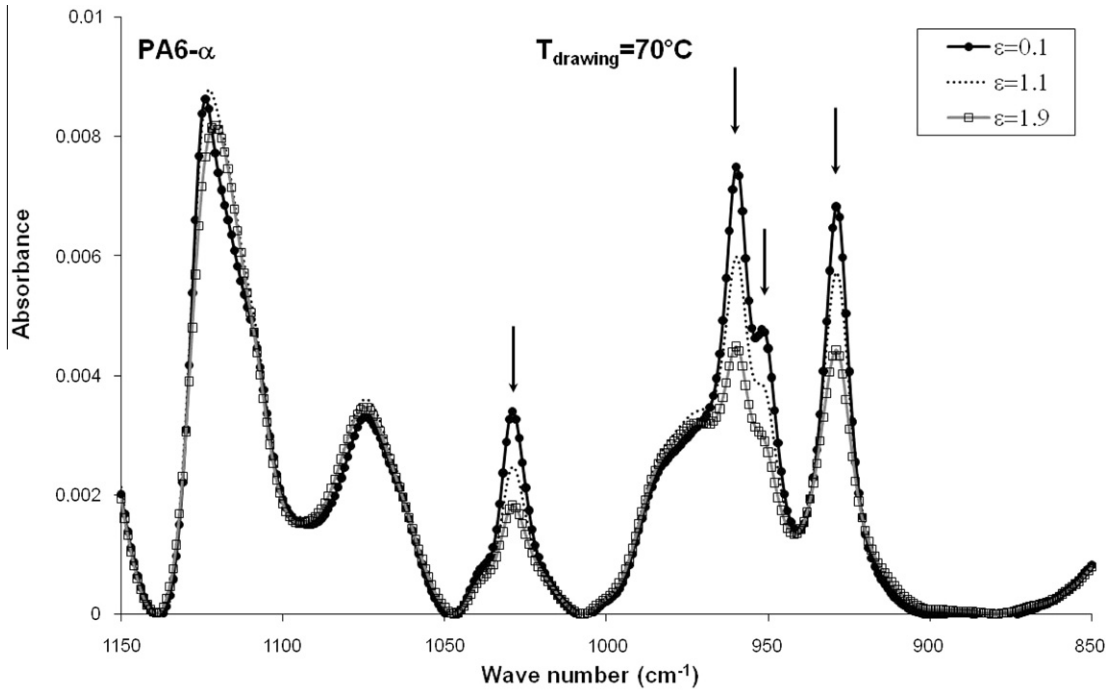

Fig. 4. Infrared spectra for αPA6 stretched at $T = 70$ °C at various strains.

Table 3
Melting point, T_m, and crystal weight fraction, X_c, for isotropic and stretched αPA6.

	T_m (°C)	X_c (%)
Isotropic	221 ± 1	30 ± 1
Stretched (70 °C; $\varepsilon = 2.1$)	220 ± 1	31 ± 1

characterized by two diffraction rings related to the (2 0 0) and (0 0 2)/(2 0 2) planes of α crystals whereas the drawn one displays two strong equatorial spots, indicating that the chains in the crystals orient towards the draw direction. The corresponding equatorial scans of both samples are depicted in Fig. 2. Deconvoluted peaks are superimposed on

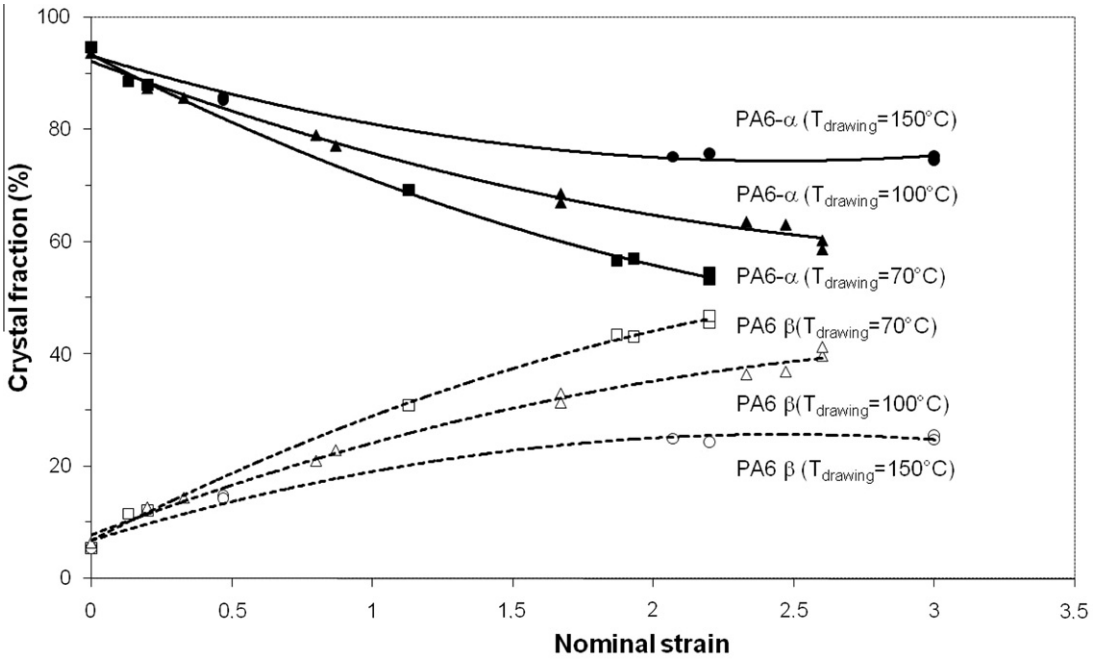

Fig. 5. Evolution of crystal fraction for αPA6 stretched at 70, 100 and 150 °C.

the experimental curve for both cases and the results from the profile analysis of the two scans are summarized in Table 1. Regarding the isotropic sample, the peak positions and the FWHM are in good agreement with results obtained by others authors for similar samples [26–27]. The observed decrease of the FWHM of the amorphous peak upon drawing is related to the orientation of the amorphous segments along the draw direction. By contrast, a significant broadening of the two crystalline peaks can be noticed. It suggests that, according to the Scherrer formula (Eq. (1)), α crystal size decreases significantly along both hydrogen bond and van der Waals bond directions, as revealed in Table 2. This means that under the present experimental conditions, plastic deformation proceeds by a large amount of α crystal breakdown, involving both $(2\,0\,0)_\alpha$ and $(0\,0\,2)_\alpha$ planes. These observations slightly differ from those reported by Argon and coworkers who have concluded that crystal breakdown occurs mostly along the (0 0 2) planes [27,28]. The origin of such discrepancies may be related to the different experimental conditions which involve different states of stress, particularly regarding hydrostatic pressure. Additionally, deformation triggers a shift towards lower Bragg angles of the (0 0 2) diffraction peak indicative of a strain-induced increase of the distance between the H-bonded sheets. This indication of the development of "defective α crystals" is further supported by the thermal study as shown in Fig. 3 which compares the thermograms of isotropic and stretched αPA6. The drawn sample exhibits a broad exotherm between 100 and 200 °C that points at structural reorganization into more stable crystals during the heating scan. This result shows that the strain induced "defective α crystals" are not thermodynamically stable and transform back into the α form, as confirmed by the melting temperature of the stretched sample. Similar exothermic phenomenon has already been discussed regarding the β–α transition [17,22].

Fig. 4 exhibits the corresponding FTIR spectra of αPA6 stretched at 70 °C as a function of deformation. The intensity of the characteristic bands of the original stable α form located at 927, 960 and 1028 cm^{-1} [29] gradually drops with increasing strain. This observation reveals the occurrence of deformation induced disorganization of the original α structure, in good agreement with the previous results by WAXS. Moreover, it is worth pointing out that the absorbance of the band at 1124 cm^{-1}, reliably attributed to the absolute amorphous content [29,30], remains roughly constant. This suggests that deformation induces crystal disorganization without global crystallinity change. The latter point is supported by DSC results, as shown in Table 3 which compares the crystal content of isotropic and stretched αPA6.

In order to elucidate the effect of drawing conditions on this order–disorder transition, all measured FTIR spectra were fitted to a linear combination of the reference spectra corresponding to PA6 in predominant α, β and γ forms. Details on this procedure have already been reported in previous papers [22,25]. Fig. 5 depicts the structural evolution as a function of strain and temperature. The most striking result is the appearance and gradual increase with increasing strain of β form. This result reveals that the "defective α phase" is akin to the mesomorphous β phase from a conformational point of view. Fig. 5 also clearly shows that the extent of the strain-induced order–disorder transition increases with decreasing *T*. The original stable α crystal phase appears to be little affected at 150 °C, in good agreement with previous work that assessed the thermomechanical stability of the α phase at $T \geqslant 150$ °C [18]. One may speculate that this finding results from a dynamic equilibrium between the mechanically induced order–disorder transition and a simultaneous thermally induced disorder–order transformation. Indeed, according to Fig. 3, the "defective α phase" starts to thermally transform into the α stable form above 100 °C.

3.2. The case of "pure" γ PA6

Fig. 6 reports the X-ray patterns of the isotropic γPA6 and a sample stretched at 70 °C. Deformation induces

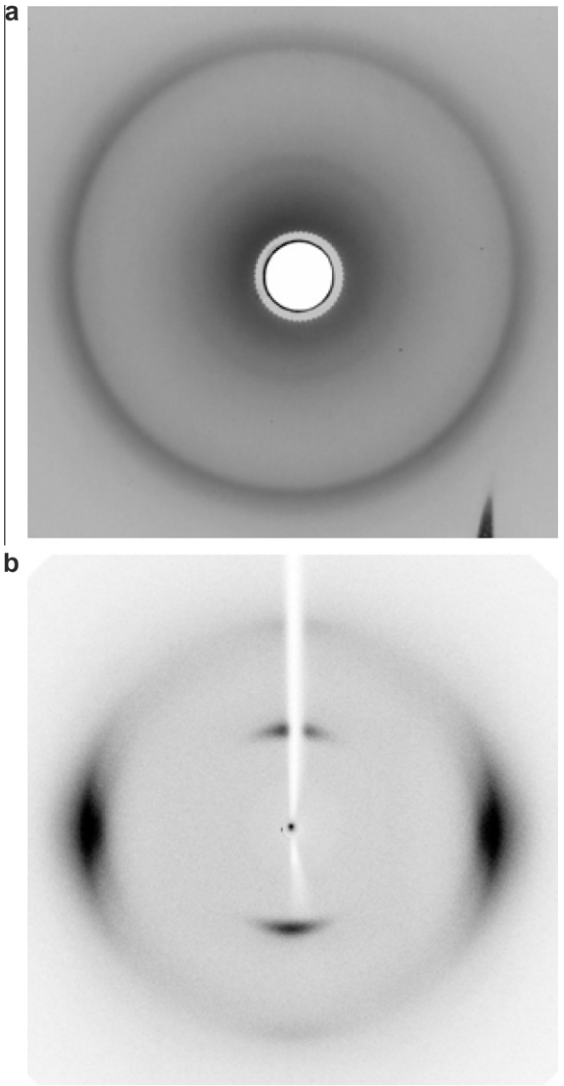

Fig. 6. X-ray patterns of γPA6 (a) isotropic and (b) stretched at 70 °C $\varepsilon = 2.4$. (vertical draw direction).

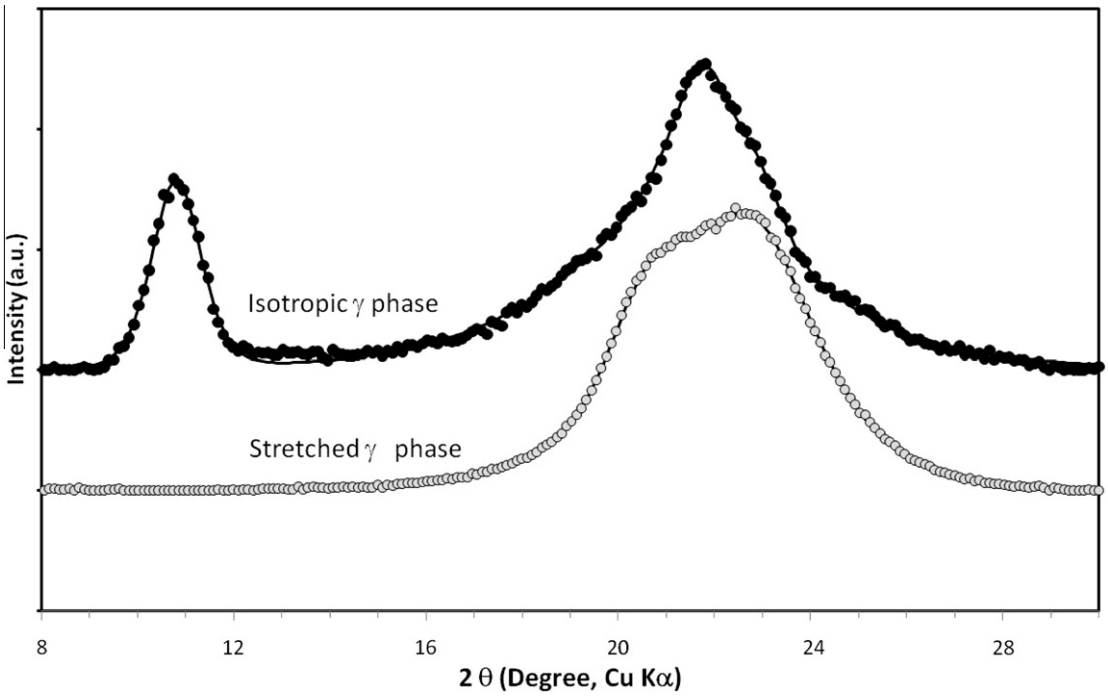

Fig. 7. Equatorial X-ray intensity profile of γPA6: (a) isotropic γPA6; (b) stretched γPA6 at 70 °C, $\varepsilon = 2.4$.

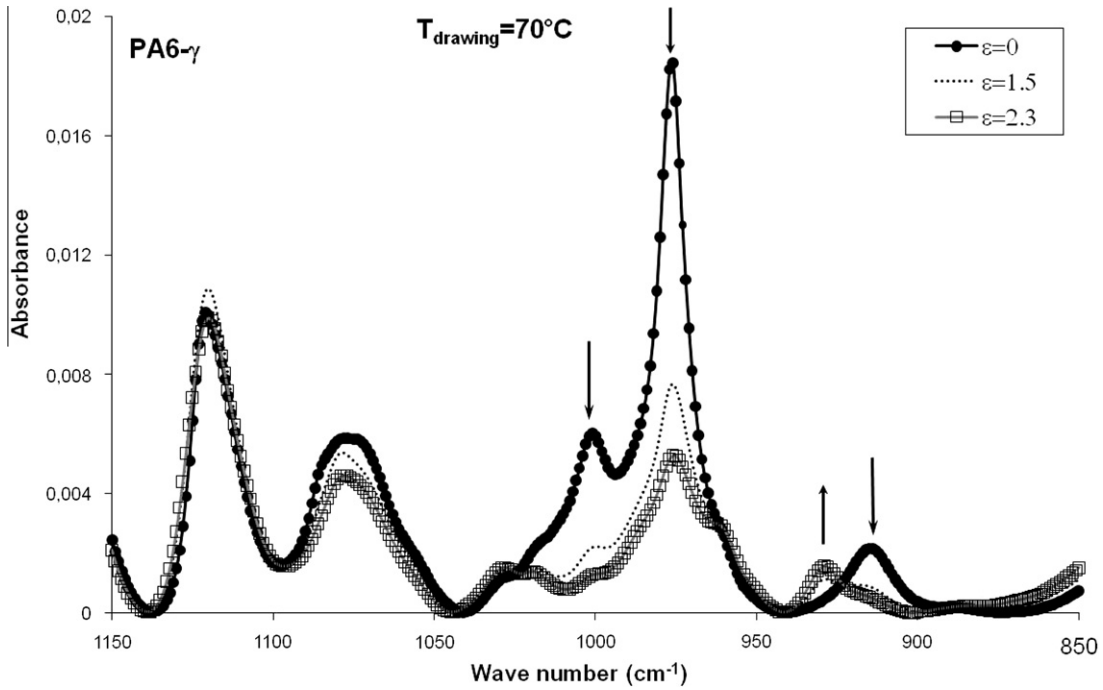

Fig. 8. Infrared spectra for γPA6 stretched at 70 °C at various strains.

Table 4
Melting point, T_m, and crystal weight fraction, X_c, for isotropic and stretched γPA6.

	T_m (°C)	X_c (%)
Isotropic	213 ± 1	31 ± 1
Stretched (70 °C; $\varepsilon = 2.4$)	221 ± 1	29 ± 1

chain orientation towards the draw direction as evidenced by the presence of the $(0\,2\,0)_\gamma$ and $(2\,0\,0)_\gamma$–$(1\,0\,0)_\gamma$ reflections in meridian and equatorial positions, respectively. The broadening of the sharp reflection in the range $20 < 2\theta < 24°$ (Figure 7), suggests crystal disordering along both *a* and *c* directions according to the γ unit cell proposed by Arimoto [11], in good agreement with Galeski's analysis [27]. In the meantime, the infrared spectra of Fig. 8 are indicative of a sharp drop of the absorption bands at 1000, 975 and 914 cm^{-1}, characteristic of the γ phase, together with the emergence of the one at 930 cm^{-1}. Again, the very faint variation band at 1124 cm^{-1} indicates that the crystal content remains almost unchanged upon drawing, confirmed by DSC results (Table 4). These results provide clear evidence for γ phase transformation into a "defective γ phase". Note that the X-ray pattern on the stretched γPA6 reported in Fig. 6b is quite similar to the one reported by Auriemma et al. for a nylon 6 fiber in mesomorphic form [16]. Fig. 9 helps clarifying the situation. The thermogram of the stretched γPA6 sample shows a broad exotherm between 120 and 190 °C relative to structural reorganization and a melting endotherm maximum located at 221 °C. For the sake of comparison, it is worth noticing that the melting points of the undeformed γ and α crystals are close to 214 and 220 °C, respectively. Moreover, it was previously established that the β phase is the only thermally unstable phase that transforms into the α phase upon heating whereas the γ form is thermally stable [17]. The thermogram of the stretched γPA6 therefore reveals that the γPA6 sample has undergone a mechanically induced γ–β phase transition, and the latter metastable phase subsequently turns back into the most stable α phase during the heating scan. Such γ−β transformation has already been observed in stretched PA6 fibres [15].

As in the case of the α phase, the effect of strain and temperature on the stability of the γ phase has been studied using quantitative FTIR data. The results are summarized in Fig. 10. For $T = 70$ °C (Fig. 10.a), a major order–disorder phase transformation occurs, leading to a largely predominant β phase in the sample prior to break. Note that the absence of experimental data in the range $0 < \varepsilon < 1.5$ is due to the fact that the γPA6 plastic deformation proceeds by necking at this temperature.

At $T = 150$ °C, a huge drop of the γ phase content to the benefit of β and α phases is observed. Close to break, the crystal structure of the stretched sample consists of both β and α forms. The strain-induced γ → α transition under uniaxial tension and under pressure is well documented in literature [18,30–34]. The present observations point at an undisclosed aspect of the kinetic process, i.e. the occurrence of a γ−β order–disorder strain-induced transition, accompanied or not of a reordering depending on the draw temperature.

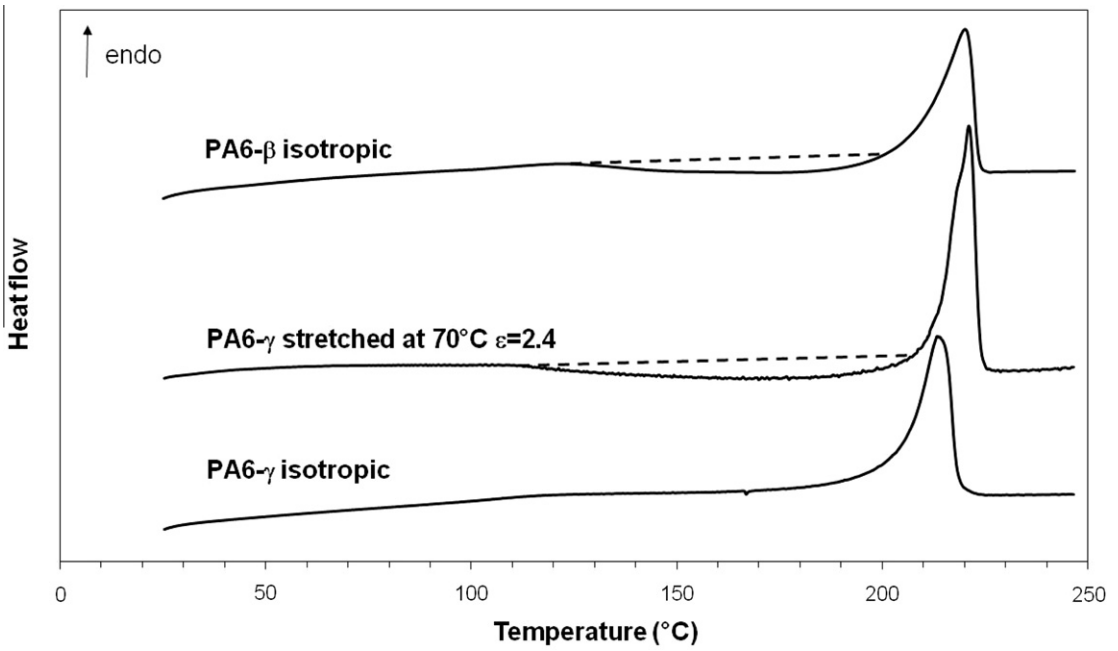

Fig. 9. DSC thermograms of γ stretched at 70 °C $\varepsilon = 2.4$ and isotropic β and γ PA6 samples.

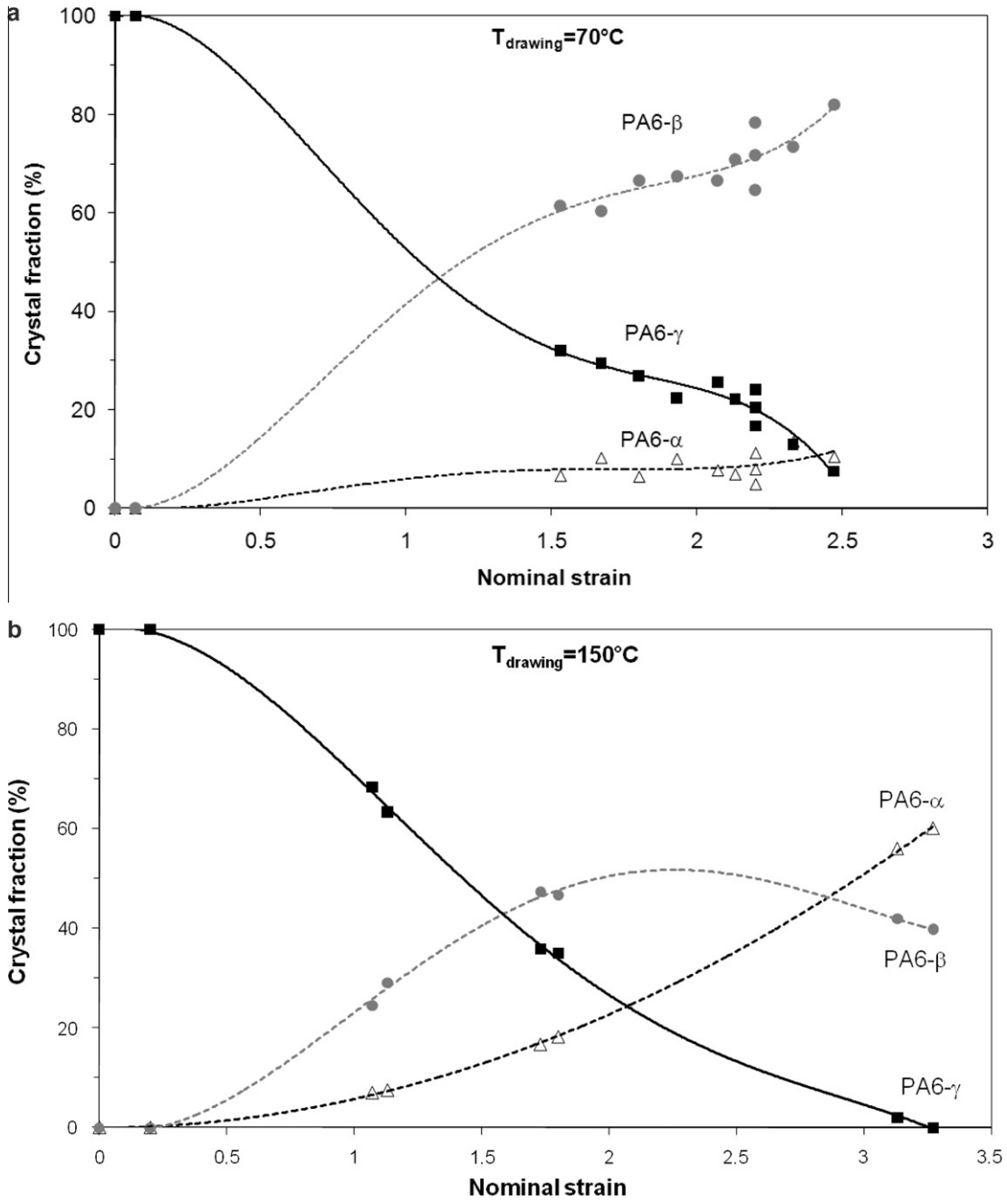

Fig. 10. Evolution of crystal fraction for γPA6 stretched at (a) T = 70 °C and (b) T = 150 °C as a function of strain.

4. Concluding remarks

Whatever the initial crystalline phase of PA6, i.e. α or γ, a strain-induced order–disorder transformation has been clearly evidenced at 70 °C, i.e. below the upper temperature limit of the viscoelastic relaxation peak associated with the glass–rubber transition whatever the crystalline phase [17]. This result is in good agreement with our previous results which have shown a close link between the strain-induced phase change and the mobility of the constrained amorphous phase.

In the case of α form, the uniaxial deformation induces a "defective α phase" that looks much like the β phase on a conformational stand point. Regarding the γ form, the strain-induced disordering gives rise to the mesomorphous β form. Various intermediate metastable crystalline phases between the perfect α and γ forms have been proposed in literature [12–16]. Some authors speculate that the

H-bonds are formed between both parallel and antiparallel chains [13,15] which mean that they are no more confined into specific planes. This destruction scheme of the original sheet-like structure provides elements of interpretation of the plastic deformation behaviour of the α and γ crystals. Indeed, the strain-induced defective structure would gradually allow for the activation of crystal slip mechanisms involving both (2 0 0) and (0 0 2) planes in the case of α and γ phases.

Previous studies focused on order–disorder phase transitions in semi-crystalline polymers have underlined the major role of chain mobility in the crystal [2,3]. It was clearly established that if drawing is performed below the temperature of the crystalline mechanical relaxation, plasticity defects may accumulate in the crystal leading to a mesomorphous phase. This phenomenon may infer a disruption of the sheet-like structure in the case of polymers containing H-bonds. This situation is encountered in the case of vinyl alcohol rich EVOH copolymers in which a strain-induced order–disorder phase transition was clearly observed in the temperature range below the crystalline α_c viscoelastic relaxation [35,36]. By contrast, if the draw temperature is above this critical temperature, chain mobility allows a continuous reorganization of the crystalline defects in the stable form.

The case of nylon 6 is however rather puzzling since it does not clearly display mechanical damping associated with chain mobility in the crystal phase. This does not mean that the crystalline phase is thoroughly deprived from such chain mobility: Murthy et al. reported on a broad transition in PA6 between 80 and 170 °C, ascribed to torsional motions of the methylene segments in the crystalline phase [37]. In view of these results, it seems that PA6 may follow the general scheme of plastic deformation depicted for several polymers such as iPP, EVOH. . .i.e. plastic deformation proceeds via partial transformation to a less ordered and less stable state if temperature is not high enough to allow for the activation of local chain rearrangements within the crystalline phase.

Acknowledgments

This work was performed with the financial support of DSM Research (Geleen, NL). Fruitful discussions with A. Stroeks, T. Brink, W. Zoetelief and A. Schmidt from DSM Research are gratefully acknowledged.

References

[1] Takahashi Y, Sumita I, Tadokoro HJ. Polym Sci, Polym Phys Ed 1973;11:2113–22.
[2] Saraf RF, Porter RS. J Polym Sci, Polym Phys Ed 1988;26:1049–57.
[3] Seguela R. J Macromol Sci Phys Rev 2005;45:263–87.
[4] Bartczak Z, Cohen RE, Argon AS. Macromolecules 1992;25:4692–704.
[5] Martins P, Nunes JS, Hungerford G, Miranda D, Ferreira A, Sencadas V, et al. Phys Lett, A 2009;373:177–80.
[6] De Rosa C, Auriemma F, Ruiz de Ballesteros O. Phys Rev Let 2006:96;167801-1-4.
[7] Saraf RF, Porter Roger S. Polym Eng Sci 1988;28:842–51.
[8] De Rosa C, Auriemma F, De Lucia G, Resconi L. Polymer 2005;46:9461–75.
[9] De Rosa C, Auriemma FJ. Am Chem Soc 2006;128:11024–5.
[10] Holmes DR, Bunn CW, Smith DJ. J Polym Sci 1955;17:159–77.
[11] Arimoto H, Ishibashi M, Hirai M, Chatani Y. J Polym Sci 1965;3:317–26.
[12] Parker JP, Lindenmeyer PH. J Appl Polym Sci 1977;21:821–37.
[13] Ziabicki A. Kolloid-Z Z Polym 1959;167(132):41.
[14] Stepaniak RF, Garton A, Carlsson DJ, Wiles DMJ. Polym Sci, Polym Phys 1979;17(987):99.
[15] Murthy NS. Polym Com 1991;32:301–5.
[16] Auriemma F, Pettraccone V, Parravicini L, Corradini P. Macromolecules 1997;30:7554–9.
[17] Penel-Pierron L, Depecker C, Seguela R, Lefebvre JMJ. Polym Sci Polym Phys 2001;39:484–95.
[18] Penel-Pierron L, Seguela R, Lefebvre J-M, Miri V, Depecker C, Jutigny M, et al. J Polym Sci Polym Phys 2001;39:1224–36.
[19] Cole KC, Depecker C, Jutigny M, Lefebvre J-M, Krawczak P. Polym Eng Sci 2004;44:231–40.
[20] Ferreiro V, Depecker C, Laureyns J, Coulon G. Polymer 2004;45:6013–26.
[21] Gurato G, Fichera A, Grandi FZ, Zannetti R, Canal P. Macromol Chem 1974;175:953–75.
[22] Miri V, Persyn O, Lefebvre JM, Seguela R, Stroeks A. Polymer 2007;48:5080–7.
[23] Wunderlich B. Macromolecular Physics, vol. 3, Crystal Melting. New York: Academic Press; 1980.
[24] Guinier A. X-ray diffraction in crystals, imperfect crystals and amorphous bodies. San Francisco: Freeman; 1963.
[25] Persyn O, Miri V, Lefebvre JM, Depecker C, Gors C, Stroeks A. Polym Eng Sci 2004;44:261–71.
[26] Murthy NS, Minor H. Polymer 1990;31:996–1002.
[27] Galeski A, Argon AS, Cohen RS. Macromolecules 1991;24:3945–52.
[28] Galeski A, Argon AS, Cohen RE. Macromolecules 1991;24:3953–61.
[29] Rotter G, Ishida H. J Polym Sci B: Polym Phys 1992;30:489–95.
[30] Vasanthan N, Salem DR. J Polym Sci Polym Phys 2001;39:536–47.
[31] Miyasaka K, Ishikawa KJ. Polym Sci 1968;6:1317–29.
[32] Murthy NS, Bray RG, Correale ST, Moore RAF. Polymer 1995;36:3863–73.
[33] Hiramatsu N, Hirakawa S. Polymer J 1982;14:165–71.
[34] Schreiber R, Veeman WS, Gabrielse W, Arnauts J. Macromolecules 1999;32:4647.
[35] Djezzar K, Penel L, Lefebvre J-M, Séguéla R, Germain Y. Polymer 1998;2:3945–53.
[36] Penel L, Djezzar K, Lefebvre J-M, Séguéla R, Fontaine H. Polymer 1998;39:4279–87.
[37] Murthy NS, Curran SA, Aharoni SM, Minor H. Macromolecules 1991;24:3215–20.